7th International Symposium on Gas Transfer at Water Surfaces IOP Publishing
IOP Conf. Series: Earth and Environmental Science **35** (2016) 012005 doi:10.1088/1755-1315/35/1/012005

The relationship between ocean surface turbulence and air-sea gas transfer velocity: An in-situ evaluation

L Esters[1], S Landwehr[1], G Sutherland[2], T G Bell[3], E S Saltzman[4], K H Christensen[5], S D Miller[6] and B Ward[1]

[1] AirSea Laboratory, NUI, Galway, Ireland
[2] Department of Mathematics, University of Oslo, Norway
[3] Plymouth Marine Laboratory, United Kingdom
[4] Department of Earth Sciences, University of California, Irvine, CA, USA
[5] Norwegian Meteorological Institute, Oslo, Norway
[6] Atmospheric Sciences Research Center, State University of New York at Albany, USA

E-mail: bward@nuigalway.ie

Abstract.

Although the air-sea gas transfer velocity k is usually parameterized with wind speed, the so-called small-eddy model suggests a relationship between k and ocean surface dissipation of turbulent kinetic energy ϵ. Laboratory and field measurements of k and ϵ have shown that this model holds in various ecosystems. Here, field observations are presented supporting the theoretical model in the open ocean. These observations are based on measurements from the Air-Sea Interaction Profiler and eddy covariance CO_2 and DMS air-sea flux data collected during the Knorr11 cruise. We show that the model results can be improved when applying a variable Schmidt number exponent compared to a commonly used constant value of 1/2. Scaling ϵ to the viscous sublayer allows us to investigate the model at different depths and to expand its applicability for more extensive data sets.

1. Introduction

Gas fluxes across the air-sea interface are computed according to:

$$F = K\ s\ \Delta P \tag{1}$$

where ΔP is the partial pressure difference of the particular gas between the ocean and the atmosphere, s is the solubility of the gas, and K is the total gas transfer velocity [1, 2]. The technology for field measurements of ΔP, of both DMS and CO_2, has matured to the point where they are readily accessible, and their values can be determined with high precision. Therefore, the main challenge remaining is to estimate K to accurately model air-sea fluxes, as K is one of the dominant sources of uncertainty in the calculation of these fluxes (e.g., [3]).

The water side air-sea gas transfer velocity k is usually parameterized as a function of wind speed ($k = f(u10)$) [4], as this is a readily available parameter from in-situ and satellite observations. However, wind speed is not the only factor influencing k. As the physical processes that influence k are mostly controlled by the near-surface dissipation rate of turbulent kinetic

energy ϵ [5], attempts have been made to directly relate k to ϵ, originally described by surface renewal models [6, 7]. These models describe the air-sea gas exchange by linking the diffusive exchange at the interface with the continuous disruption of the diffusive boundary layer due to turbulent motions. Higher turbulence means more frequent renewal of the water side boundary layer and thus a higher gas exchange rate. Lamont and Scott [8] suggest to model this relation using the small-eddy model:

$$k = A\,\mathrm{Sc}^{-n}(\epsilon_0\ \nu)^{1/4} \tag{2}$$

where A is a proportionality constant, ϵ_0 the dissipation rate of TKE at the air-sea interface, Sc is the Schmidt number, which is defined as the ratio of the kinematic viscosity of water ν to mass diffusivity of water D so, $\mathrm{Sc} = \nu/D$, and n is the Schmidt number exponent. For the surface renewal models, Lamont and Scott [8] predicted a Schmidt number exponent of $n = 1/2$. This Schmidt number exponent of $n = 1/2$ is not applicable for interfaces covered with surfactants. For film-covered surfaces, a Schmidt number exponent of $n = 2/3$ is found [9]. In reality, sea surfaces might be partially covered with surfactants and n varies between $1/2$ for a wavy surface and $2/3$ for a flat surface depending on the sea surface conditions [10, 11]. Laboratory experiments [12, 13] and field measurements [14, 15, 16, 17] of k and ϵ have shown that this theoretical relation agrees with observations, and that ϵ is a good predictor of gas transfer in various ecosystems. These studies cover various types of environmental systems and range from tank experiments to lakes, rivers, estuaries, and coastal oceans as well as the model-world Biosphere 2 [14, 15, 16, 17]. In addition, these studies cover various types of environmental forcing like wind, tides, and rain and were measured using a variety of instrumentation. This variety of observational setups and environments demonstrates the universality of the small-eddy model described in equation 2.

All these studies show a high correlation between k and ϵ, though significant variation is found in the empirical proportionality coefficient A (equation 2), usually calculated through linear regression. As the turbulence measurements were carried out at various depths below the surface, the differences in A are most likely related to this, as ϵ strongly depends on depth in the surface region of the ocean [18]. Another source of variability in A is the sea surface condition as well as surfactants at the sea surface (e.g., [12]), but Tokoro *et al.* [15] argue that this should affect ϵ and not A. Wang *et al.* [17] evaluated the small-eddy model under non-breaking wave conditions based on turbulence measurements directly below the sea surface. Their results indicate that A scales linearly with $\log(\epsilon)$ and they show that the relation holds for other published studies focusing on similar environments (i.e., lakes with wind and wave-induced surface turbulences), and in laboratory experiments. However, this relation contradicts the measurements of Zappa *et al.* [14], which were taken in different environmental systems with different forcing.

To the best of our knowledge, no investigations have been performed in the open ocean relating k to ϵ. Measurements of eddy covariance CO_2 and DMS air-sea fluxes and of ϵ from the Air-Sea Interaction Profiler (ASIP), taken during the Knorr11 cruise, provide an opportunity to investigate the relation between k and ϵ in the open waters of the North Atlantic Ocean.

2. Methods

Measurements were taken during a field campaign in the North Atlantic, aboard the R/V *Knorr* from late June to mid-July 2011 leaving and returning to Woods Hole, USA [19, 20, 21, 22, 23].

2.1. Flux measurements

The 3D wind speed was measured at 10 Hz with two Csat3 sonic anemometers mounted at the bow mast of the R/V *Knorr*. The measurements were corrected for ship motion as described in Miller *et al.* [24] and Landwehr *et al.* [25]. The time series of the motion corrected wind

speeds were used to calculate the air-side friction velocity u_{*_a} and the trace gas fluxes. The CO_2 fluctuations were measured at 10 Hz with a non-dispersive infra-red gas analyzer of the brand LICOR. A diffusion dryer was used to remove ambient water vapor fluctuations [26]. It was shown in Landwehr *et al.* [27] that this significantly improves the quality of the direct CO_2 flux measurements. The DMS flux measurements and data analysis are described in Bell *et al.* [28]. The total gas transfer velocities K of CO_2 and DMS were calculated using equation 1 based on 10-min averaged measured data. These K-values combine the effects of processes at the air as well as the water side of the air-sea interface. The water side gas transfer velocity k was calculated and normalized to a Schmidt number of 660 (CO_2 at 25°C):

$$k_{660} = k \cdot \left(\frac{660}{\mathrm{Sc}_x}\right)^{-0.5} \tag{3}$$

where Sc_x refers to the Schmidt number at the in situ seawater state for either DMS or CO_2.

2.2. ASIP

Presented here are data from four deployments (a total of 283 profiles) of ASIP, an autonomous upwardly rising microstructure profiler. ASIP, which is extensively described in Ward *et al.* [29], is equipped with a variety of sensors and ϵ is calculated from two shear probes. To validate the small-eddy model only the surface values of ϵ are of interest. As the vertical resolution of the measured ϵ is approximately 0.5 m, all data points within the uppermost 0.5 m of the ocean are declared as surface values ($\epsilon_{0.5}$). These surface values of ϵ are compared to the measured k_{660} based on the DMS and CO_2 flux measurements (in the following called k_{DMS} and k_{CO_2}).

2.3. Scaling ϵ

It is not straightforward to measure ϵ at the air-sea interface and there is little open-ocean data of near-surface ϵ available. Therefore, it is helpful to scale ϵ close to the air-sea interface, once a universal relation between ϵ and k is determined. Lorke and Peeters [5] took the approach to consider the oceanic boundary layer as a shear-driven, flat surface, and scaled ϵ with the *law of the wall* (LOW) [30]. The underlying assumption of this approach is that the total stress in the boundary layer is constant, which leads to a log-linear velocity profile:

$$\epsilon(z) = \frac{u_{*_w}^3}{\kappa z} \tag{4}$$

where $\kappa \approx 0.41$ is the von Kármán constant, z is the distance down from the ocean surface, and u_{*_w} is the measured water side friction velocity. The applicability of the assumption that the sea surface is purely shear driven is questioned [31, 32, 33, 34]. Measurements show that higher dissipation rates can be found than those predicted by the LOW. These higher rates are usually ascribed to breaking waves [31, 32, 33]. The results of this study show that the scaled ϵ are nevertheless well correlated to the measured ϵ from ASIP. By comparing the scaled and measured surface ϵ an offset between them was determined. The profiles of ϵ were extrapolated to the viscous sublayer thickness, which has been shown to be a function of wind speed [35, 36]. The relationship from Wu [37] was used to determine this thickness, given by $z_\nu = 11\nu/u_{*_w}$, and an offset was subtracted to yield the dissipation rate at the interface (ϵ_0). These interface values are on average two orders of magnitude higher than the actual measured $\epsilon_{0.5}$ in the uppermost 0.5 m of the ocean.

2.4. Schmidt number exponent

All mentioned field studies on the small-eddy model assumed a constant Schmidt number exponent of $n = 1/2$ for the full range of their measurements [14, 15, 16]. However, n depends

on the sea surface conditions and is known to vary between 1/2 for a wavy sea surface to 2/3 for a smooth surface [10, 11]. Krall [38] carried out experiments investigating the dependence of n on wind speed for different surfactant coverage in the Aeolotron at the university in Heidelberg. During these experiments, Krall [38] distinguished between three surface conditions: clean surface, 0.052 mmol/l Triton and 0.26 mmol/l Triton, and determined different $n(u_{10})$ relations for each of them (figure 1). The higher the surfactants coverage, the higher is the wind speed at which n reaches 2/3, and the steeper is the wind speed dependence.

Neither the surfactant coverage nor the mean square slope were measured during Knorr11, so n was parameterized based on wind speed at 10 m height (u_{10}) only. It is assumed that a medium surfactant coverage prevailed during Knorr11, as there were several instances of high chlorophyll values.

The best fit of $n(u10)$ was determined for k_{DMS} and for k_{CO_2} based on equation 2 with the assumption that the proportionality would be unity ($A = 1$). The best fit for $n(u_{10})$ based on k_{DMS} is $n = -0.259\log(u_{10}) + 0.83$ and $n = -0.162\log(u_{10}) + 0.642$ based on k_{CO_2}. For both gases a logarithmic fit best described the relationship over a linear fit. Overall, the relation based on k_{DMS} yielded better results (RMSD ± 4.3 cm hr^{-1}) than the one based on k_{CO_2} (RMSD ± 21.5 cm hr^{-1}) due to less variability in k_{DMS} measurements. According to figure 1, $n(u10)$ reaches the upper limit at a similar wind speed to the one for medium surfactants [38] and follows its trend whilst being less steep.

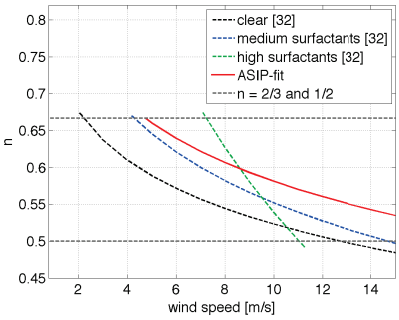

Figure 1. The Schmidt number exponent n versus wind speed based on Krall [38] for high surfactant coverage (0.26 mmol/l Triton in green), medium surfactant coverage (0.052 mmol/l Triton in blue), clean surface (black), and the best fit between the measured ϵ and k_{DMS} in the small-eddy model during Knorr11 (red). The grey colored lines give the theoretical boundaries of $n = 1/2$ and $n = 2/3$.

3. Results and discussion

To improve the statistics, the ASIP data are averaged over 90 minutes. Figure 2a and 2b show the results of applying $n = f(u10)$ instead of a constant $n = 1/2$ value in equation 2. For $n = f(u10)$, 89% of the variation in k_{DMS} can be explained by the small-eddy model, compared to 53% for a constant n. The k_{CO_2} data are more variable than k_{DMS} (figure 2c and 2d). For $n = 1/2$, R^2 is found to be 0.16, whereas for $n = f(u10)$, $R^2 = 0.2$. For both gases, DMS and CO_2, k is highly variable at low wind speeds, and thus higher n.

The proportionality coefficient A, which is found through data regression, has to be adapted when applying $n(u10)$ instead of a constant $n = 1/2$. Figure 2b shows that $A = 1.0 \pm 0.11$ for k_{DMS}, which is reasonable as the parametrization of $n(u10)$ is based on the assumption that $A = 1$ in equation 2. For the commonly used $n = 1/2$ a proportionality of $A = 0.42 \pm 0.05$ is observed for k_{DMS}. This value is nearly identical to the theoretical value of 0.4 [8] and close to values found in field experiments of Zappa *et al.* [14] ($A = 0.419 \pm 0.130$), whose depth measurements for ϵ ranged from a few cm to 3 m below the sea surface. Vachon *et al.* [16] estimated $A = 0.44 \pm 0.01$ for large lakes and $A = 0.39 \pm 0.02$ for smaller lakes measuring ϵ at 10 cm depth by using the floating chamber method. Thus, when applying the same assumptions as in these studies in lakes, rivers, and estuaries, similar results are obtained in the open ocean.

The proportionality constant A for $n = 1/2$ (k_{DMS}) is, however, approximately double that of Tokoro *et al.* [15], who determined values of $A = 0.13$ to 0.2 at depths scaled to 86 cm and

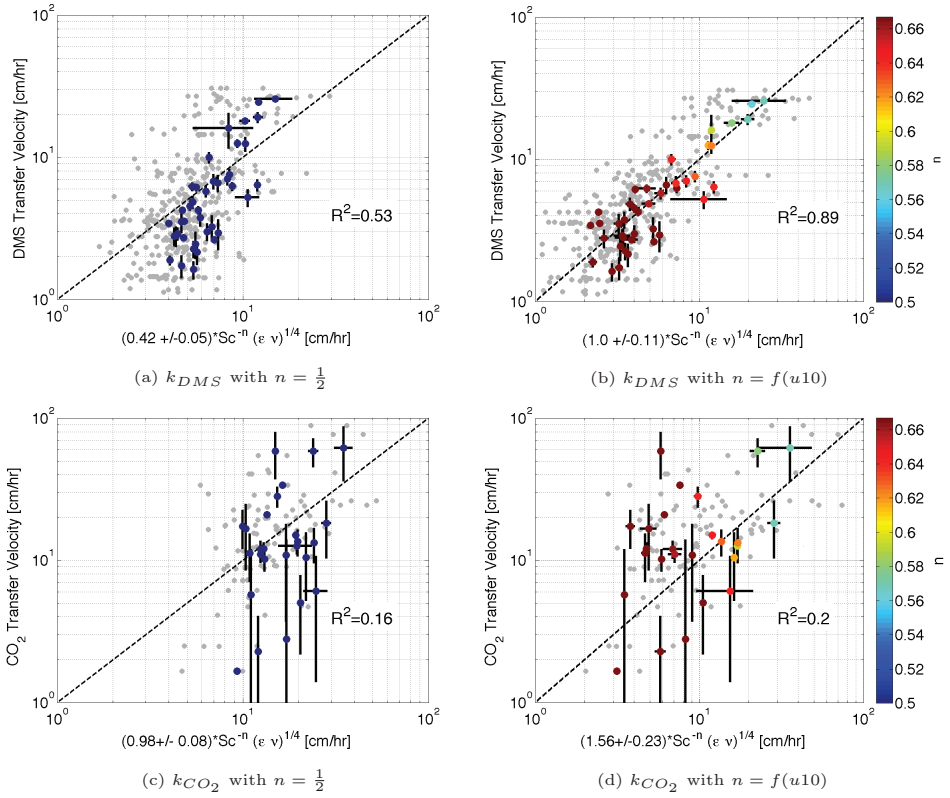

(a) k_{DMS} with $n = \frac{1}{2}$ (b) k_{DMS} with $n = f(u10)$

(c) k_{CO_2} with $n = \frac{1}{2}$ (d) k_{CO_2} with $n = f(u10)$

Figure 2. Ninety-minute averaged k and the prediction of the small-eddy model based on measured ϵ taken within the uppermost 0.5 m ($\epsilon_{0.5}$) of the ocean in log–log space. The color code represents n, the errors bars show the standard error of k (std/sample size$^{1/2}$), the grey data in the background are the non-averaged data, and the dashed line represents the 1:1 relation.

also double that of Wang *et al.* [17], who report values of $A = 0.25$ measured at 0.25 cm depth and $A = 0.31$ at 10 cm depth. To further investigate this variability in A, the measured ϵ are extrapolated closer to the air-sea interface (the viscous sublayer). These scaled and extrapolated values of ϵ feature 6% less variability than those originally measured. This reduction in variability might explain the higher coefficient of determination R^2 at the interface compared to the total uppermost 0.5 m (figure 2 compared to figure 3). For $n = f(u10)$, the small-eddy model explains 91% of the variability in k_{DMS} at the interface (ϵ_0) and 69% for $n = 1/2$. Again, the relation between k_{CO_2} and the right-hand side of the small-eddy model is lower than for k_{DMS}, and the small-eddy model explains only 18% of the variability for $n = 1/2$ and 19% for $n = f(u10)$.

For k_{DMS} as well as for k_{CO_2}, the determined A have lower values when scaled to the air-sea interface compared to the measurements at 0.5 m (0.18 ± 0.03 for $n = 1/2$ and 0.39 ± 0.06 for $n(u10)$ based on k_{DMS}, and 0.31 ± 0.09 for $n = 1/2$ and 0.47 ± 0.15 based on k_{CO_2}). The value of A for k_{DMS} with $n = 1/2$ at the interface is significantly closer to those reported by Wang *et al.* [17] measured at 0.25 cm depth than the A found for the same setting within the whole surface layer. This supports the idea that A depends on the depth of the turbulence measurements, where A has to follow the $\epsilon(z)$ dependency to balance the small-eddy model.

Once a parametrization for $n(u10)$ and a corresponding A are determined, the small-eddy model is applicable to more extensive gas transfer datasets. This approach can be used to predict k by figure of ϵ being scaled based on LOW and thus based on u_{*_w} instead of real ϵ measurements. Figure 4 shows the prediction of the small-eddy model for the complete Knorr11

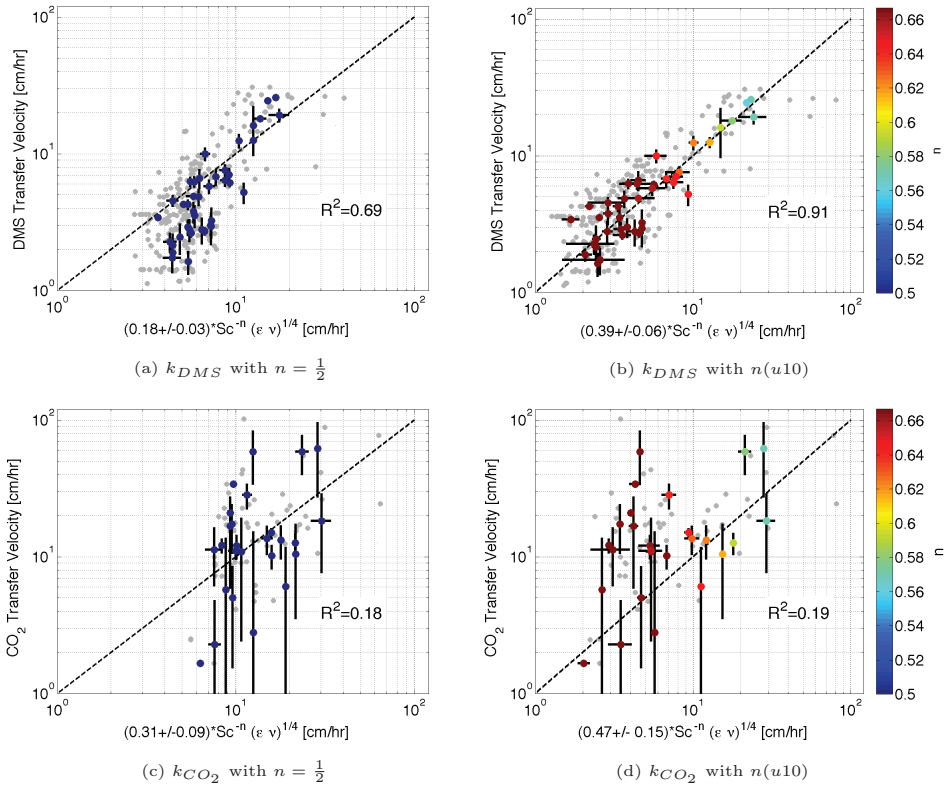

(a) k_{DMS} with $n = \frac{1}{2}$ (b) k_{DMS} with $n(u10)$

(c) k_{CO_2} with $n = \frac{1}{2}$ (d) k_{CO_2} with $n(u10)$

Figure 3. Ninety-minute averaged k and the prediction of the small-eddy model based on $\epsilon(z)$ predicted by the LOW (equation 4), fitted to the measured ϵ profiles and extrapolated to the viscous sublayer depth ϵ_0 ($z_\nu = 11\nu/u_{*_w}$). The colour code represents n, the errors bars show the standard error of k (std/sample size$^{1/2}$), the grey data in the background are the non-averaged data, and the dashed line represents the 1:1 relation.

data [20].

Bin averaging k reduces variability and results in a linear relationship between k_{CO_2} and the right hand side of equation 2, with a R^2 value of 0.92. For k_{DMS} a lower correlation is found, as there is a deviation in the transfer velocity at high wind speeds, which has been explained by Bell *et al.* [20]. If these data points are ignored ($u10 > 12$ m/s), R^2 reaches 0.78, so the small-eddy model explains a large part of the variability in k_{DMS} for low and medium wind speeds.

No measurements of ϵ exist at high wind speeds during Knorr11 (indicated in figure 4). Therefore, a reduction in ϵ during high wind speeds could explain the discrepancy between the predicted k_{DMS} and the measured one (figure 4). A reduction in ϵ with a simultaneous increase in bubbles could also explain the different behavior in k_{DMS} and k_{CO_2} [20].

4. Conclusions

Various studies on gas exchange across the air-sea interface, including a variety of methods and techniques ranging from theoretical approaches to laboratory studies to field campaigns in lakes, coastal areas and estuaries, have verified ϵ to be a good predictor for k using the small-eddy model [5, 12, 13, 14, 15, 16]. Our measurements of k and ϵ verify that this theoretical relation holds well in the open ocean.

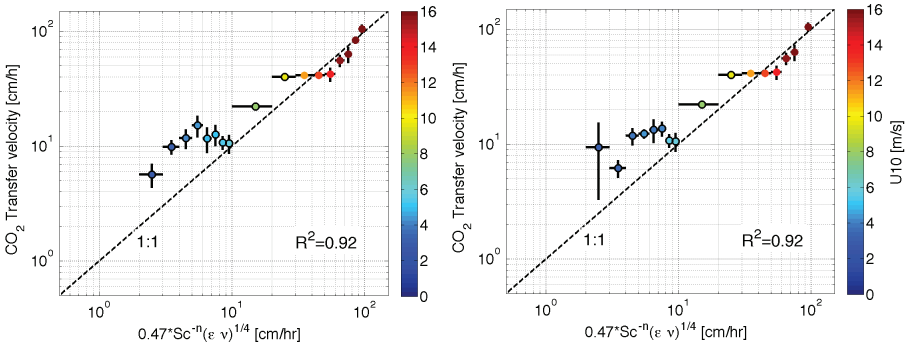

(a) k_{DMS} (b) k_{CO_2}

Figure 4. Bin-averaged measured k against the u_{*_w}-based prediction (LOW in equation 4) of the small-eddy model for the full Knorr11 data. Values of ϵ_0 are predicted by the LOW for the viscous sublayer depth ($z_\nu = 11\nu/u_*$) with a determined offset between measurements and predictions being subtracted. For the small-eddy model a varying Schmidt number exponent $n = f(u10)$ is applied. Only the circled data points indicate bins in which more than three actual turbulence measurements exist. For wind speeds higher than 12 m/s, we do not have any direct measurements of ϵ. The colour code represents the wind speed, the errors are given by the standard error of k (std/bincounts$^{1/2}$) and the dashed line represents the 1:1 relation.

When applying the same assumption that $n = 1/2$, as in former studies, the small-eddy model explains 53% of the variability in k_{DMS} and only 16% of the variability in k_{CO_2}. Our field data show that this relation can be significantly improved when applying a varying Schmidt number exponent n. This n is know to vary with the sea surface conditions. A parametrization for n based on wind speed improves the predictability of the small-eddy model to 89% for k_{DMS}. This $n = f(u10)$ changes the right-hand side of equation 2 similar to the approach of Wang *et al.* [17], who scale the proportionality coefficient with $A \propto log(\epsilon)$. In both cases, the expression is shifted towards lower values for low ϵ and vice versa.

Wang *et al.* [17] report different logarithmic parameterizations of A for different depths to retain a linear relation for the small-eddy model. The parametrization of $n = f(u10)$ presented here, however, is universal for different depth levels. In this case, the constant A has to only be adapted for each depth level to avoid any offset in the linear relation between both sides of the small-eddy model. Thus our results support the idea that A depends on depth, and increases towards the air-sea interface as A has to balance the increase in ϵ towards the interface. Measurements of ϵ reported in earlier studies on this topic were taken at various depths, which makes comparisons of A difficult.

Surface conditions and the function for n (either a constant or $n = f(u_{10})$) impact values of A. Once an appropriate function for n and a corresponding A for the depth of interest is found, a universal relation between k and ϵ can be determined.

In this work the LOW is used to scale ϵ from depth measurements to the air-sea interface, but future work will involve the implementation of different scaling approaches to predict ϵ [21].

Acknowledgments

Leonie Esters gratefully receives support from the NUIG College of Science Fellowship Programme. The attendance of the GTWS-7 was supported by the Marine Institute Networking and Travel Grant, the Ryan Institute Travel Support Scheme, and the GTWS-7 travel support scheme. Funding for the Knorr11 field experiment was supported by Science Foundation Ireland under grant number 08/US/I1455 and the EU FP7 project CARBOCHANGE under grant

agreement no. 264879.

References

[1] Weiss R F 1974 Carbon dioxide in water and seawater: The solubility of a nonideal gas *Mar. Chem.* **2** 203–215
[2] Wanninkhof R, Asher W E, Ho D T, Sweeney C and McGillis W R 2009 Advances in Quantifying Air–Sea Gas Exchange and Environmental Forcing *Ann. Rev. Mar. Sci.* **1** 213–244
[3] Johnson M T, Hughes C, Bell T G and Liss P S 2011 A Rumsfeldian analysis of uncertainty in air-sea gas exchange *Gas Transfer at Water Surfaces 2010* ed Komori S, McGillis W and Kurose R (Kyoto, Japan: Kyoto University Press.) pp 464–484
[4] Wanninkhof R 1992 Relationship between wind speed and gas exchange over the ocean *J. Geophys. Res.* **97** 7373–7382
[5] Lorke A and Peeters F 2006 Toward a Unified Scaling Relation for Interfacial Fluxes *J. Phys. Oceanogr.* **36** 955–961 10.1175/JPO2903.1
[6] Higbie R 1935 The rate of absorption of a pure gas into a still liquid during short periods of exposure *AlChE J.* **31** 365–389
[7] Danckwerts P V 1951 Significance of liquid film coefficients in gas absorption *Ind. Eng. Chem.* **43** 1460–1467
[8] Lamont J C and Scott D S 1970 An eddy cell model of mass transfer into the surface of a turbulent liquid *AlChE J.* **16** 513–519
[9] Davies J T 1972 *Turbulence phenomena* (Academic Press., N.Y.)
[10] Deacon E L 1977 Gas transfer to and across an air–water interface *Tellus* **29** 363–374
[11] Jähne B, Henz G and Dietrich W 1987 Measurement of the diffusion coefficients of sparingly soluble gases in water *J. Geophys. Res.* **92** 10767–10776
[12] Asher W and Pankow J F 1986 The interaction of mechanically generated turbulence and interfacial films with a liquid phase controlled gas/liquid transport process *Tellus B* **38** 305–318
[13] Moog D B and Jirka G H 1999 Air-Water Gas Transfer In Uniform Channel Flow *J. Hydraul. Eng.* **125** 3–10
[14] Zappa C J, McGillis W R, Raymond P A, Edson J B, Hintsa E J, Zemmelink H J, Dacey J W H and Ho D T 2007 Environmental turbulent mixing controls on air–water gas exchange in marine and aquatic systems *Geophys. Res. Lett.* **34** L10601
[15] Tokoro T, Kayanne H, Watanabe A, Nadaoka K, Tamura H, Nozaki K, Kato K and Negishi A 2008 High gas–transfer velocity in coastal regions with high energy-dissipation rates *J. Geophys. Res.* **113** C11006
[16] Vachon D, Prairie Y T and Cole J J 2010 The relationship between near–surface turbulence and gas transfer velocity in freshwater systems and its implications for floating chamber measurements of gas exchange *Limnol. Oceanogr.* **55** 1723–1732
[17] Wang B, Liao Q, Fillingham J H and Bootsma H A 2015 On the coefficients of small eddy and surface divergence models for the air–water gas transfer velocity *J. Geophys. Res. Oceans* **120** 2129–2146
[18] Sutherland G, Ward B and Chrisensen K H 2013 Wave–turbulence scaling in the ocean mixed layer *Ocean Sci.* **9** 597–608
[19] Scanlon B and Ward B 2013 Oceanic wave breaking coverage seperation techniques for active and maturing whitecaps *Methods Oceanogr.* **8** 1–12
[20] Bell T G, De Bruyn W, Miller S D, Ward B, Christensen K H and Saltzman E S 2013 Air–sea dimethylsulfide (DMS) gas transfer in the North Atlantic: evidence for limited interfacial gas exchange at high wind speed *Atmos. Chem. Phys.* **13** 11073–11087
[21] Sutherland G, Christensen K H and Ward B 2013 Wave-turbulence scaling in the ocean mixed layer *Ocean Sci.* **9** 597–608
[22] Christensen K H, Röhr J, Ward B, Fer I, Broström G, Sætra Ø and Breivik Ø 2013 Surface wave measurements using ship mounted ultrasonic altimeter *Method Oceanogr.* **6** 1–15
[23] Sutherland G, Christensen K H and Ward B 2014 Evaluating langmuir turbulence in the oceanic boundary layer *J. Geophys. Res.* **119** 1899–1910
[24] Miller S, Marandino C, van de Bruyn W and Saltzman E S 2009 Air-sea gas exchange of co_2 and dms in the north atlantic by eddy covariance *Geophys. Res. Lett.* **36** L15816
[25] Landwehr S, O'Sullivan N and Ward B 2015 Direct Flux Measurements from Mobile Platforms at Sea: Motion and Airflow Distortion Corrections Revisited *J. Atmos. Oceanic Technol.* **32** 1163 – 1178
[26] Miller S D, Marandino C and Saltzman E S 2010 Ship-based measurement of air-sea CO_2 exchange by eddy covariance *J. Geophys. Res.* **115** D02304
[27] Landwehr S, Miller S D, Smith M J, Saltzman E S and Ward B 2014 Analysis of the pkt correction for direct co_2 flux measurements over the ocean *Atmospheric Chemistry and Physics* **14** 3361–3372
[28] Bell T G, Bruyn W D, Miller S D, Ward B, Christensen K and Saltzman E S 2013 Air/sea DMS gas transfer

in the North Atlantic: evidence for limited interfacial gas exchange at high wind speed *Atmos. Chem. Phys.* 11073–11087
[29] Ward B, Fristedt T, Callaghan A H, Sutherland G, Sanchez X, Vialand J and tenDoeschate A 2014 The air–sea interaction profiler for microstructure measurements in the upper ocean *J. Atmos. Oceanic Technol.* **31** 2246–2267
[30] Callaghan A H, Ward B and Vialard J 2014 Influence of surface forcing on near-surface and mixing layer turbulence in the tropical indian ocean *Deep-Sea Res.* **4**
[31] Kitaigorodskii S A, Donelan M A, Lumley J L and Terray E A 1983 Wave–Turbulence Interactions in the Upper Ocean. Part II. Statistical Characteristics of Wave and Turbulent Components of the Random Velocity Field in the Marine Surface Layer *J. Phys. Oceanogr.* **13** 1988–1999
[32] Agrawal Y C, Terray E A, Donelan M A, Hwang P A and Williams III A J 1992 Enhanced dissipation of kinetic energy beneath surface waves *Nature* **359** 219–220
[33] Terray E A, Donelan M A, Agrawal Y C, Drennan W M, Kahma K K, Williams III A J, Hwang P A and Kitaigorodskii S A 1996 Estimates of Kinetic Energy Dissipation under Breaking Waves *J. Phys. Oceanogr.* **26** 792–807
[34] Babanin A V and Haus B K 2009 On the Existence of Water Turbulence Induced by Nonbreaking Surface Waves *J. Phys. Oceanogr.* **39** 2675–2679
[35] Ward B and Donelan M A 2006 Thermometric measurements of the molecular sublayer at the air–water interface *Geophys. Res. Lett.* **33** L07605
[36] Ward B 2007 *Transport at the Air Sea Interface — Measurements, Models and Parameterizations* ed Garbe C S, Handler R A and Jähne B (Springer Verlag)
[37] Wu J 1971 An estimation of oceanic thermal–sublayer thickness *J. Phys. Oceanogr.* **1** 284–286
[38] Krall K E 2013 *Laboratory Investigations of Air-Sea Gas Transfer under a Wide Range of Water Surface Conditions* (PhD. Ruperto-Carola University of Heidelberg, Germany)